Ancient TL

An improved multiple-aliquot regenerative-dose (MAR) procedure for post-IR IRSL dating of K-feldspar

Bo Li[1*], Zenobia Jacobs[1,2], Richard G. Roberts[1,2]

[1] Centre for Archaeological Science, School of Earth and Environmental Sciences
University of Wollongong, New South Wales, Australia
[2]ARC Centre of Excellence for Australian Biodiversity and Heritage, University of Wollongong,
Wollongong, NSW 2522, Australia

*Corresponding Author: bli@uow.edu.au
Received: March 19, 2017; in final form: May 7, 2017

Abstract

In optical dating, multiple-aliquot dating methods have been considered inferior to single-aliquot methods, due to difficulties inherent to in between-aliquot normalisation. In this study, we propose an improved multiple-aliquot regenerative-dose (MAR) procedure for the multiple-elevated-temperature post-IR IRSL (MET-pIRIR) signals from K-feldspar grains. This method is based on observations that a common, or standardised, growth curve (SGC) exists between different aliquots from the same and different samples, and that between-aliquot variation can be largely eliminated by application of regenerative-dose ('re-normalisation') or least squares (LS) normalisation procedures. We find that this improved MAR procedure significantly increases the accuracy and precision of D_e determinations. We tested this method using several sediment samples from Marathousa, a Middle Pleistocene archaeological site in Greece, and demonstrate that, for the K-feldspar grains from these samples, the proposed MAR method overcomes problems associated with inappropriate sensitivity correction of the natural (L_n) and test dose (T_n) signals at low stimulation temperatures (50 – 150 °C) more effectively than the SAR method. The MAR method can also reduce instrument time for measurement of older samples.

Keywords: K-feldspar, IRSL, post-IR IRSL, multiple aliquot, single aliquot

1. Introduction

In optical dating, both the optically stimulated luminescence (OSL) signal from quartz and infrared stimulated luminescence (IRSL) signal from potassium-rich (K) feldspar grains can be measured to determine the radiation ('burial') dose received by mineral grains after their last exposure to sunlight (Aitken, 1998). To obtain useful information regarding the burial time of quartz and K-feldspar grains, the OSL or IRSL signals must be converted into a reliable estimate of equivalent dose (D_e). The D_e is estimated by comparing the natural OSL or IRSL signals against a series of known-dose laboratory signals that form a dose response curve (DRC); regenerative-dose methods are preferred over additive-dose methods, because the D_e is obtained by interpolation, rather than by extrapolation, of the DRC (e.g., Lian & Roberts, 2006). Two kinds of regenerative-dose methods have been developed for D_e determination—multiple-aliquot regenerative-dose (MAR) procedures (Wintle, 1993; Aitken, 1998) and single-aliquot regenerative-dose (SAR) procedures (Murray & Roberts, 1998; Galbraith et al., 1999; Murray & Wintle, 2000). Emphasis has shifted from the development and use of MAR procedures to SAR procedures to exploit the many inherent advantages of the latter (e.g., Duller, 2008; Wintle, 2014).

Some studies, however, have demonstrated that the SAR method is not always suitable, and that there may be merit in revisiting the MAR procedure in specific cases. For example, for quartz samples from the Chinese Loess Plateau, Lu et al. (2007) showed that the build-up of OSL signal during repeated SAR measurement cycles resulted in underestimation of the D_e. They proposed a sensitivity-corrected MAR method, in which the test dose signal (T_x) is used to normalise between aliquots, following the suggestion by

Roberts & Duller (2004) that T_x not only corrects for sensitivity change but can also be used for between-aliquot normalisation. In the MAR procedure of Lu et al. (2007), the sensitivity-corrected natural signal (L_n/T_n) was projected on to the dose response curve established using the sensitivity-corrected regenerative-dose signal (L_x/T_x) from multiple aliquots.

For feldspar IRSL signals, it has been suggested that a large sensitivity change may occur during measurement of L_n, resulting in a significant difference between the luminescence efficiency of the natural dose and subsequent test dose (T_n), and between L_n/T_n and L_x/T_x, when using SAR (e.g., Chen et al., 2013; Li et al., 2013a; Chen et al., 2015; Guo et al., 2015; Van den Bergh et al., 2016). This would cause the sensitivity correction of L_n to be inappropriate, giving rise to erroneous D_e estimates. Li et al. (2013a) were the first to apply a MAR procedure based on sensitivity-corrected signals (L_n/T_n and L_x/T_x) to pIRIR dating of K-feldspar grains. In their study, the sample was divided into different groups of aliquots: one group was used to measure the natural signals, and the other groups were bleached using a solar simulator for several hours before being given different regenerative doses. The IRSL and MET-pIRIR L_x and T_x signals were then measured to establish a dose response curve, and the D_e estimated from the L_n/T_n signals. A similar approach was adopted by Chen et al. (2015) and Guo et al. (2015). This method, however, is only suitable for samples that exhibit homogeneous behaviours among different aliquots, and is not applicable to samples with L_x/T_x signals that are highly variable among different grains or aliquots (e.g., Li et al., 2014b, 2015b).

A key objective of any MAR procedure, therefore, should be to reduce any between-aliquot variability. This can be achieved through the application of an appropriate normalisation procedure. Li et al. (2015a, 2016) proposed the regenerative-dose normalisation ('re-normalisation') and least squares (LS) normalisation methods to reduce the between-aliquot differences in DRC shapes for single aliquots of quartz and K-feldspar. When these methods were applied to samples from a variety of geological provenances, environmental settings and depositional ages, the OSL and MET-pIRIR signals had significantly reduced between-aliquot scatter and similar DRCs. As a result, a 'global standardised growth curve' (gSGC) could be established for quartz (Li et al., 2015a, 2016) and K-feldspar (Li et al., 2015b).

In this study, we aim to investigate the feasibility of incorporating the re-normalisation method into a MAR procedure, and examine the advantages and disadvantages of the new MAR procedure compared to conventional MAR and SAR procedures. We demonstrate that the new MAR method overcomes the difficulty in normalising for between-aliquot scatter in samples from a site in Greece, and allows for the construction of a standardised growth curve for these samples. This method has the potential to be used for D_e determination of K-feldspars from other sites and geographical locations.

2. Sample descriptions

Samples were collected from Marathousa I, a newly discovered Lower Palaeolithic archaeological site located in the Megalopolis basin in southern Greece (Panagopoulou et al., 2015). The sedimentary deposits are of Middle Pleistocene age and are composed of lacustrine clay, silt and sand beds, alternating with lignite seams, representing a former lake environment (Vinken, 1965; Van Vugt et al., 2000). Here, we present results for four samples: MAR-01, MAR-R1, MAR-R2 and MAR-R5. MAR-01, MAR-R2 and MAR-R5 were collected from sandier units underlying the archaeological level, while MAR-R1 was collected from a lignite seam overlying the archaeological level.

3. Experimental procedures

All samples were prepared for IRSL analysis using routine procedures (Aitken, 1998). Samples were treated with solutions of HCl acid and H_2O_2 to remove carbonates and organic matter, respectively, and then dried and sieved to obtain grains of 180 – 212 μm in diameter. The K-feldspar grains were separated from quartz and heavy minerals using a solution of sodium polytungstate with a density of 2.58 g/cm^3. The separated K-feldspar grains were immersed in 10 % HF acid for 40 min to etch the surfaces of the grains and remove the outer, alpha-irradiated portions; they were then rinsed in HCl acid to remove any precipitated fluorides. The dried and etched K-feldspar grains were mounted as a monolayer on stainless-steel discs of 9.8 mm diameter using "Silkospray" silicone oil as an adhesive. Grains covered the central ∼ 5 mm diameter portion of each disc, corresponding to several hundred grains per aliquot.

IRSL measurements were made on an automated Risø TL-DA-20 reader equipped with IR diodes for stimulation (870 △ 40 nm). The total IR power delivered to the sample position was ∼ 135 mW/cm^2 (Bøtter-Jensen et al.,

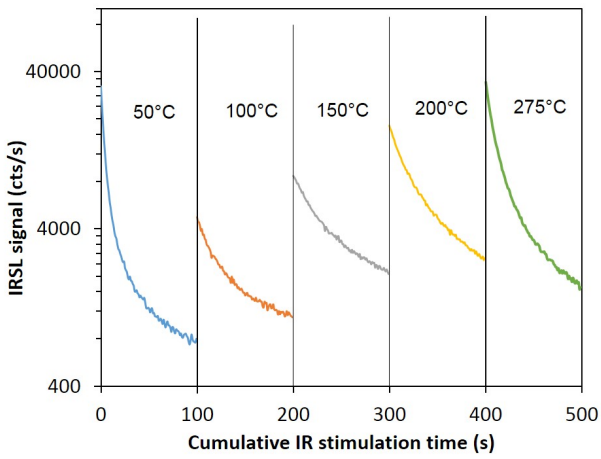

Figure 1. Representative IRSL (50 °C) and MET-pIRIR (100 – 275 °C) decay curves for a single aliquot of sample MAR-01, stimulated at different temperatures (shown above each curve).

Table 1. Single-aliquot (a) and multiple-aliquot (b) procedures for pMET-pIRIRmeasurements.

Step	Treatment		Observed
	(a) Single-aliquot	(b) Multiple-aliquot	
1	Give regenerative dose, D_i [a]	Give regenerative dose, D_i [a]	
2	Preheat at 320 °C for 60 s	Preheat at 320 °C for 60 s	
3	[b] IRSL measurement at 50 °C for 100 s	[b] IRSL measurement at 50 °C for 100 s	L_x (50 °C)
4	[b] IRSL measurement at 100 °C for 100 s	[b] IRSL measurement at 100 °C for 100 s	L_x (100 °C)
5	[b] IRSL measurement at 150 °C for 100 s	[b] IRSL measurement at 150 °C for 100 s	L_x (150 °C)
6	[b] IRSL measurement at 200 °C for 100 s	[b] IRSL measurement at 200 °C for 100 s	L_x (200 °C)
7	[b] IRSL measurement at 275 °C for 100 s	[b] IRSL measurement at 275 °C for 100 s	L_x (275 °C)
8	Give test dose, 60 Gy	Give test dose, 60 Gy	
9	Preheat at 320 °C for 60 s	Preheat at 320 °C for 60 s	
10	[b] IRSL measurement at 50 °C for 100 s	[b] IRSL measurement at 50 °C for 100 s	T_x (50 °C)
11	[b] IRSL measurement at 100 °C for 100 s	[b] IRSL measurement at 100 °C for 100 s	T_x (100 °C)
12	[b] IRSL measurement at 150 °C for 100 s	[b] IRSL measurement at 150 °C for 100 s	T_x (150 °C)
13	[b] IRSL measurement at 200 °C for 100 s	[b] IRSL measurement at 200 °C for 100 s	T_x (200 °C)
14	[b] IRSL measurement at 275 °C for 100 s	[b] IRSL measurement at 275 °C for 100 s	T_x (275 °C)
15	**Solar simulator bleach for 4 hrs**	**Solar simulator bleach for 4 hrs**	
16	Repeat step 1–15 for different D_i	Give normalisation dose, D_r [b]	
17		Preheat at 320 °C for 60 s	
18		[b] IRSL measurement at 50 °C for 100 s	L_r (50 °C)
19		[b] IRSL measurement at 100 °C for 100 s	L_r (100 °C)
20		[b] IRSL measurement at 150 °C for 100 s	L_r (150 °C)
21		[b] IRSL measurement at 200 °C for 100 s	L_r (200 °C)
22		[b] IRSL measurement at 275 °C for 100 s	L_r (275 °C)
23		Give test dose, 60 Gy	
24		Preheat at 320 °C for 60 s	
25		[b] IRSL measurement at 50 °C for 100 s	T_r (50 °C)
26		[b] IRSL measurement at 100 °C for 100 s	T_r (100 °C)
27		[b] IRSL measurement at 150 °C for 100 s	T_r (150 °C)
28		[b] IRSL measurement at 200 °C for 100 s	T_r (200 °C)
29		[b] IRSL measurement at 275 °C for 100 s	T_r (275 °C)

[(a)] For the natural sample, the given dose $D_i = 0$ Gy

[(b)] The same D_r ($\sim$ 400 Gy) is applied to all aliquots from the different groups.

2000). Laboratory irradiations were carried out on the reader using a calibrated $^{90}Sr/^{90}Y$ beta source. IRSL signals were detected by an Electron Tubes Ltd. 9235B photomultiplier tube fitted with Schott BG-39 and Corning 7-59 filters to restrict transmission to 320 – 480 nm. Each IRSL measurement was made for 100 s, and the resulting signal was calculated as the sum of counts over the initial 10 s of optical stimulation, with 'late light' subtraction (Aitken, 1998) of the background count rate over the final 10 s of optical stimulation. For each IRSL measurement, an 'IR-off' period of up to 50 s prior to stimulation was applied to monitor and minimise the isothermal decay signal (Fu et al., 2012).

4. Results

4.1. A single-aliquot LS-normalisation procedure and standardised growth curve

We tested whether the LS-normalisation method is applicable to the samples from Greece, using a total of 18 single aliquots of K-feldspar from sample MAR-01. Each aliquot was measured using the SAR pMET-pIRIR procedure (Table 1a), in which the aliquots were bleached for $\sim$ 4 hrs in a solar simulator at the end of each SAR cycle (Li et al., 2014b). Two to four regenerative doses, ranging from 0 to $\sim$ 1900 Gy, were given to each aliquot and the signals measured, together with the signals arising from the test dose of $\sim$ 60 Gy applied to each aliquot. Fig. 1 shows representative natural IRSL (50 °C) and MET-pIRIR (100 – 275 °C) decay curves for an aliquot of sample MAR-01. The intensities of the MET-pIRIR signals are on the order of a few hundred to several tens of thousands of counts per second. The L_n/T_n and L_x/T_x signals observed for different aliquots of this sample, measured at different stimulation temperatures, are compared in Fig. 2a – e. Large between-aliquot scatter can be observed: for example, the relative standard deviation (RSD) of the L_x/T_x ratios at a fixed dose are about 5 – 10 %. This finding is similar to that made by Li et al. (2015b), who suggested that T_x cannot fully correct for the differences between aliquots.

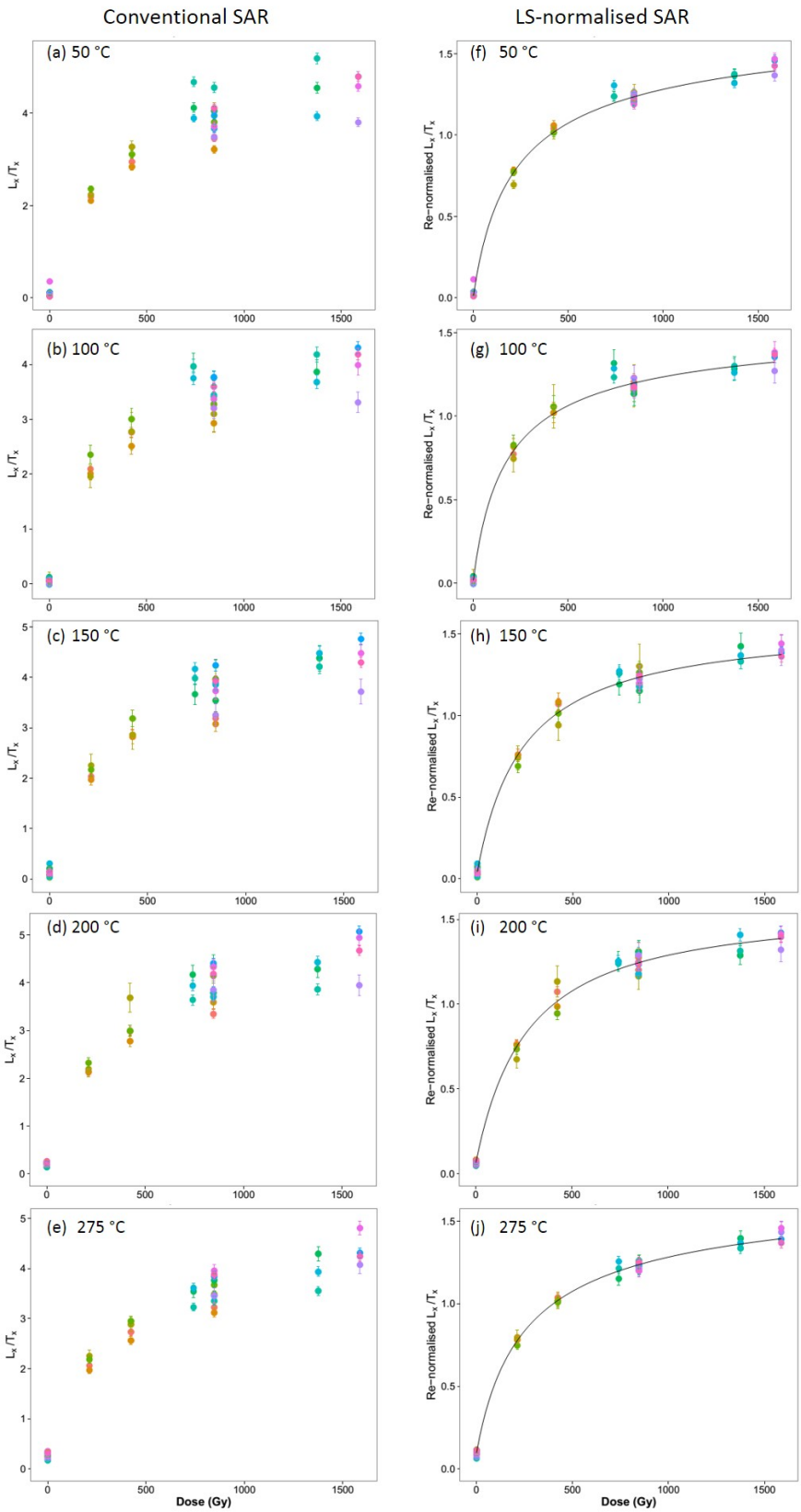

Figure 2. SAR L_x/T_x ratios (a – e) and re-normalised L_x/T_x ratios (f – j) for sample MAR-01, plotted as a function of laboratory dose. Different aliquots are represented by different colours. Aliquots were measured using the SAR pMET-pIRIR listed in Table 1a. The data shown in panels (f) – (j) for the different aliquots were fitted using a general-order kinetic function (full lines). The DRCs have been normalised to unity at a dose of 400 Gy, to facilitate direct comparison with the multiple-aliquot DRCs (section 4.3).

To test whether different aliquots of the same sample have similar growth curve shapes, we applied the LS-normalisation procedure of Li et al. (2016). This procedure comprises the following steps: (1) L_x/T_x signals from all aliquots are fitted using a best-fit model; (2) L_x/T_x values from each aliquot are re-scaled using scaling factors determined through an optimisation procedure that minimises the sum of squared residuals between the re-scaled signals and the curve of best fit; and (3) the fitting (step 1) and re-scaling (step 2) procedures are repeated iteratively until there is negligible change in the LS-normalised regenerative-dose signals. The LS-normalisation procedure was achieved using the built-in function 'lsNORM()' provided in the **R**-package 'numOSL' (Peng et al., 2013; R Core Team, 2016). A general-order kinetic (GOK) function (Guralnik et al., 2015) of the form $f(x) = a[1-(1+bcx)^{(-1/c)}]+d$, where x is the dose and the parameters a, b, c and d are constants, was used to fit the DRCs; a denotes the maximum signal level, b is the reciprocal of the saturation dose D_0, c is a kinetic order modifier, and d is an offset accounting for potential recuperation effects. For $c \to 0$, the GOK function reduces to a single saturating exponential. As c increases, the GOK function progressively deviates from first-order behaviour and approximates a double saturating exponential or a saturating exponential plus linear function; see Guralnik et al. (2015) for details.

The LS-normalised DRCs are shown in Fig. 2f – j, where it can be seen that the between-aliquot scatter for the L_x/T_x ratios is greatly reduced (e.g., the RSD for the L_x/T_x signals at a fixed dose is reduced to about 1 – 4 %). These results suggest that different aliquots measured using the SAR pMET-pIRIR procedure share similar DRCs, provided the L_x/T_x signals are normalised appropriately.

4.2. A multiple-aliquot LS-normalisation procedure and standardised growth curve

We propose that the MAR procedure can also be improved and optimised using this LS-normalisation method. The two most critical prerequisites of a multiple-aliquot procedure are that: 1) different aliquots share the same DRCs; and 2) between-aliquot differences in luminescence signals are normalised appropriately. For the former, we have demonstrated that the pMET-pIRIR signals from feldspars may share similar DRCs (Li et al., 2015b), and this is confirmed for our samples (section 4.1). For between-aliquot normalisation, we applied the pMET-pIRIR procedure of Li et al. (2013a, 2014b) to all four Greek samples. A total of 55 aliquots (4 from MAR-01, 15 from MAR-R1, 22 from MAR-R2 and 14 from MAR-R5) were bleached in the solar simulator for $\sim$ 8 hrs. These aliquots were then given different regenerative doses, ranging from 0 to $\sim$ 2000 Gy, and were measured using the procedure listed in Table 1b. The IRSL signals for the regenerative and test doses were measured successively at 50, 100, 150, 200 and 275 °C, following a preheat at 320 °C for 60 s. At the end of each test dose IRSL measurement, the aliquots were bleached for $\sim$ 4 hrs in a solar simulator. An identical regenerative dose (D_r) was then given to the bleached aliquots, followed by measurement of the regenerative and corresponding test dose signals (L_r and T_r, respectively), as before.

The L_x/T_x ratios measured at different stimulation temperatures are shown in Fig.3a – e for different aliquots, plotted against their corresponding regenerative doses. Two features of these data are noteworthy. First, there are large between-sample variations in the L_x/T_x ratios at a dose. Second, there is also substantial between-aliquot scatter for some of these samples. As a result, a reliable DRC cannot be constructed from the multiple-aliquot L_x/T_x ratios. Fig.3f – j shows the re-normalised ratios ($\frac{L_x/T_x}{L_r/T_r}$), plotted as a function of regenerative dose at the different stimulation temperatures. The L_x/T_x ratios were normalised by dividing the corresponding L_r/T_r ratios obtained by giving each aliquot an additional regenerative dose, D_r (Table 1b). Peng et al. (2016) conducted numerical simulations comparing the SGCs obtained using different re-normalisation doses and found little difference in accuracy or precision for a range of re-normalisation doses; we used a re-normalisation dose of 400 Gy for our samples. It can be seen that the between-aliquot scatter is reduced and, more importantly, the normalisation procedure appears to bring the DRCs of the different samples into much closer alignment. This result supports our proposition that the re-normalisation procedure can help improve the MAR results, to the extent that there is potential to construct reliable SGCs for multiple-aliquot MET-pIRIR signals.

4.3. Comparing LS-normalised SAR and MAR SGCs

The fitted SAR SGCs shown in Fig. 2f – j are shown as red dashed lines in Fig. 3f – j, to facilitate comparison with the MAR SGCs, shown as solid lines. Both the SAR and MAR SGCs were normalised using the signal induced by a regenerative dose of 400 Gy, so their shapes are directly comparable. The SAR SGCs differ from the MAR SGCs at low stimulation temperatures (i.e., 50, 100 and 150 °C); they exhibit a much steeper growth at low doses and reach a slightly higher saturation level (Fig. 3f – h). The difference is most significant for the 50 °C IRSL signal (Fig. 3f) and decreases as the stimulation temperature is increased. Only a slight difference in DRC shape and saturation intensity is observed at a stimulation temperature of 275°C (Fig. 3j). We propose that the difference between the SAR and MAR SGCs at the lower temperatures is a result of progressive sensitivity change (luminescence efficiency) between the measurement of L_x and T_x, possibly extending over several measurement cycles for different IR stimulation temperatures. A prediction of this outcome is that the D_e values determined using the SAR and MAR SGCs are likely also to be different, especially for the signals measured using low-temperature stimulations.

4.4. D_e estimation based on SAR and MAR SGCs

We calculated D_e values based on the SAR SGCs for each stimulation temperature (Fig. 2f – j), following the method

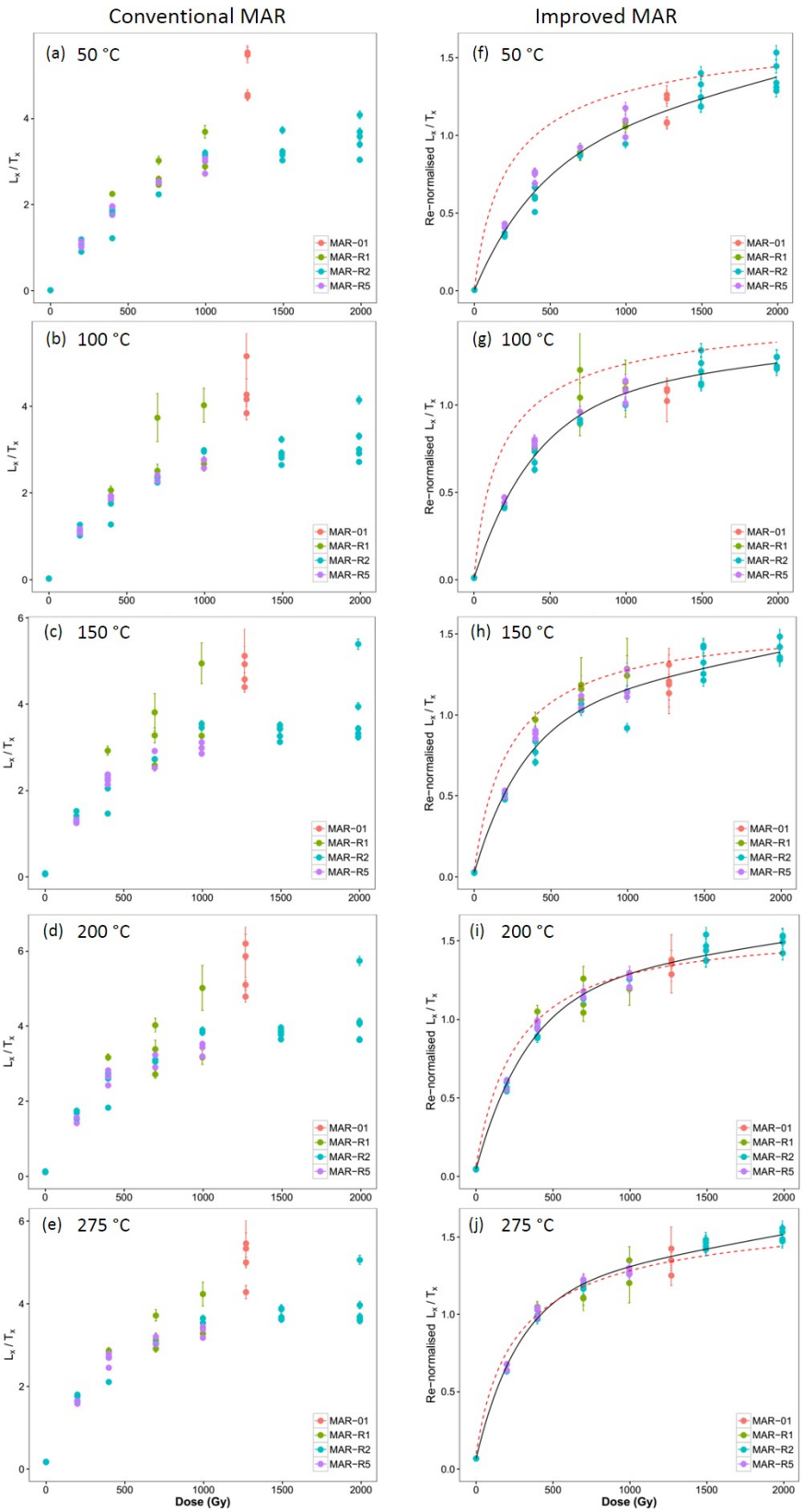

Figure 3. MAR L_x/T_x ratios (a – e) and re-normalised MAR L_x/T_x ratios (f – j) for the four Greek samples, plotted as a function of laboratory dose. Each data point corresponds to one aliquot, with different colours representing the different samples. The data shown in panels (f) – (j) were fitted using a general-order kinetic function, shown by black lines; the dashed lines are the best-fit SGCs obtained from the SAR data for sample MAR-01 (Fig.2f – j).

and equation presented in Li et al. (2015a):

$$f(D_e) = \frac{L_n}{T_n} \times \frac{f(D_r)}{\frac{L_r}{T_r}}$$

where $f(D_e)$ denotes the SAR SGCs established by LS-normalisation, and D_r and L_r/T_r denote the additional regenerative dose and the ratio for the corresponding sensitivity-corrected signal, respectively. Li et al. (2015a) provide a worked example of how to calculate SGC D_e values using this function.

We also calculated D_e values based on the MAR SCGs at each stimulation temperature (Fig. 3f – j) for three of the samples — MAR-01 (6 aliquots), MAR-R2 (9 aliquots) and MAR-R5 (10 aliquots) — using the pMET-pIRIR procedure listed in Table 1b. After measuring the L_n and T_n signals, each aliquot was bleached for $\sim$ 4 hrs in the solar simulator and then given a regenerative dose of 400 Gy and a subsequent test dose of 60 Gy, the same as used to establish the MAR SGCs. The L_n/T_n ratios were then re-normalised using the corresonding (L_r/T_r) ratios, and the re-normalised ratios ($\frac{L_n/T_n}{L_r/T_r}$) were projected on to the MAR SGCs (solid lines in Figs. 3f – j) to estimate the D_e values.

The D_e values determined at each stimulation temperature were combined using the central age model (Galbraith et al., 1999; Galbraith & Roberts, 2012) (to obtain weighted-mean D_e values for the single- and multiple-aliquot data sets, for comparison. The weighted-mean D_e values are plotted as a function of stimulation temperature in Fig. 4a – c (D_e-T plots) for samplesMAR-01, MAR-R2 and MAR-R5. The MAR D_e values (circles) differ negligibly with stimulation temperature, whereas the SAR D_e values (triangles) increase systematically with stimulation temperature, resulting in statistically significant differences between the SAR and MAR weighted-mean D_e values for all three samples at stimulation temperatures of 50, 100 and 150 °C. The SAR and MAR weighted-mean D_e values are statistically indistinguishable at stimulation temperatures of 200 and 275 °C.

Low-temperature (<200 °C) IRSL signals are commonly thought to suffer from anomalous fading, giving rise to underestimation of the measured D_e values (Li et al., 2014a). The D_e-T plot is often used in support of this influence (Li & Li, 2011), based on observations of an increase D_e with an increase in stimulation temperature until a D_e 'plateau' is reached at higher temperatures; the latter is interpreted as indicating negligible fading of the IRSL signal at stimulation temperatures above 200 °C (Li & Li, 2011) or above 250 °C for older samples (Li & Li, 2012). The SAR D_e-T plots exhibit patterns for the Greek samples consistent with those reported previously for other samples (i.e., an increase in D_e with stimulation temperature), which might be attributed to anomalous fading causing underestimation of the measured D_e values at low stimulation temperatures. However, the MAR D_e-T plots show negligible change in D_e with an increase in stimulation temperature, which implies no difference in fading rate of the signals measured at the various stimulation temperatures.

To explicitly test for the effect of fading on D_e values,

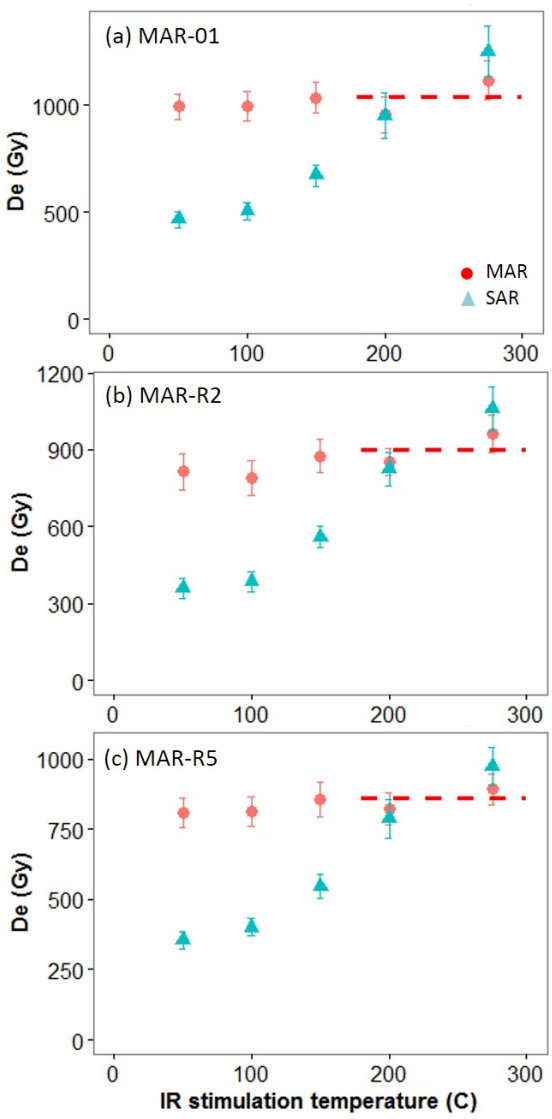

Figure 4. D_e values obtained based on SAR SGCs (blue triangles) and MAR SGCs (red circles), plotted as a function of IR stimulation temperature for samples MAR-01 (a), MAR-R2 (b) and MAR-R5 (c). The horizontal dashed lines represent the weighted-mean SAR and MAR D_e values obtained at IR stimulation temperatures of 200 and 275 °C.

we conducted anomalous fading tests on samples MAR-R2 and MAR-R5, using a single-aliquot measurement procedure similar to that described in Auclair et al. (2003), but based on the MET-pIRIR procedure. The corresponding anomalous fading rates (g-values) are displayed in Fig. 5a for the IRSL and MET-pIRIR signals measured at the different stimulation temperatures. There is little difference between the fading rates for the various signals, and all g-values are statistically consistent with zero at 2σ. This pattern differs from those reported for samples from other regions, as presented in previous studies, which typically exhibit the highest anomalous fading rate for the 50 °C IRSL signal and lower rates for the signals measured at higher stimulation temperatures (e.g., Li

& Li, 2011, 2012). Given the absence of significant fading in samples MAR-R2 and MAR-R5, therefore, the D_e values should be consistent regardless of stimulation temperature, and this is confirmed by the MAR D_e results.

Furthermore, the fading test results indicate that the pattern seen in the SAR D_e results is not a result of varying degrees of anomalous fading at the different stimulation temperatures. Instead, we suggest that this pattern indicates that the extents of sensitivity changes occurring during measurement of L_n, prior to measurement of T_n, are different from those occurring between L_x and T_x, so that the sensitivity-correction method in SAR does not adequately compensate for these changes. This proposition is supported by the SAR dose recovery data for sample MAR-01 (Fig. 5b), which display the same pattern of increasing D_e with increasing stimulation temperature as seen with the natural samples (Fig. 4a – c), i.e., there are significant underestimation in the recovered ratio for the low-temperature (50 – 100 °C) signals. Given anomalous fading is not a factor in dose recovery experiments, the underestimation in the low-temperature (50 – 100 °C) signals confirms that the pattern seen in the SAR D_e results is a result of different extents of sensitivity changes occurred during measurement of L_n, T_n, L_x and T_x.

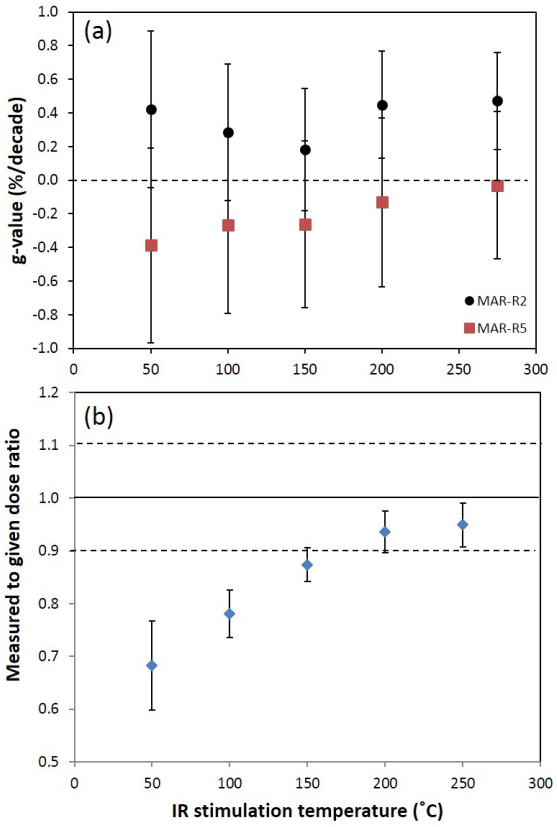

Figure 5. (a) Anomalous fading rates (expressed as the g-value) for samples MAR-R2 (black cirles) and MAR-R5 (red squares), plotted against IR stimulation temperature. (b) SAR dose recovery test results for sample MAR-01, obtained using the pMET-pIRIR procedure listed in Table 1a.

5. Discussion

The new LS-normalised pMET-pIRIR MAR method applied to K-feldspar offers several advantages over standard SAR procedures. Most importantly, it does not suffer from problems associated with inappropriate sensitivity correction between measurement of the L_n, T_n and L_x and T_x signals. Similar to previous studies (e.g., Chen et al., 2013; Li et al., 2013b; Chen et al., 2015; Guo et al., 2015; **?**), we find that erroneous results can be obtained using a SAR procedure if the relative change in sensitivity between L_n and T_n is significantly different from the changes between L_x and T_x. Our SGC (Fig. 3f – j), fading (Fig. 5a), dose recovery test (Fig. 5b) and D_e (Fig. 4) results demonstrate that the MAR method proposed here can circumvent this problem effectively. Additionally, the MAR method potentially requires less instrument time than the SAR method, especially for older samples that need more and larger regenerative doses to construct a robust DRC. A MAR SGC can be established using different samples from the same site (Fig. 3), so there is no need to measure the same regenerative doses for each sample, and a single MAR SGC can be used to estimate D_e values for samples spanning a range of ages from the same site. Furthermore, the results produced by this method should be more reliable, because a DRC established using more regenerative doses (or data points) will be more precise than a conventional SAR dose response curve and also more resistant to random errors caused by measurement uncertainties, which may result in significant changes to the shape of observed DRCs (Li et al., 2017). As with all DRCs, it is important to minimise any sources of possible systematic bias in the construction of SGCs.

6. Conclusions

We have proposed a LS-normalised MAR procedure to determine D_e values for K-feldspars using the pMET-pIRIR signal. Our method is built on the demonstration that a common growth curve, or SGC, exists for different pIRIR signals (Li et al., 2015b) and that between-aliquot variation can be largely eliminated by normalising the L_n/T_n and L_x/T_x ratios using the corresponding L_r/T_r ratios from an additional regenerative dose (Li et al., 2015b,b, 2016). By applying a re-normalisation procedure, the new MAR method can overcome the main drawback of conventional multiple-aliquot methods — the difficulty of normalising different aliquots — resulting in a significant improvement in the accuracy and precision of the DRC construction and D_e estimation. Problems associated with inappropriate sensitivity correction of the L_n signal using the T_n signal in the standard SAR procedure can also be avoided and, especially for older samples, instrument time can be saved.

Acknowledgments

This research was funded by the Australian Research Council through Future Fellowships to Li (FT140100384) and Jacobs (FT150100138), and an Australian Laureate Fellowship to Roberts (FL130100116). We thank Yasaman Jafari and Terry Lachlan for valuable support in the OSL dating laboratory, and Panagiotis Karkanas for advice and assistance in the field.

References

Aitken, M.J. *An Introduction to Optical Dating*. Oxford University Press, 1998.

Auclair, M., Lamothe, M., and Huot, S. *Measurement of anomalous fading for feldpsar IRSL using SAR*. Radiation Measurements, 37 (4-5): 487–492, 2003.

Bøtter-Jensen, L., Bulur, E., Duller, G.A.T., and Murray, A.S. *Advances in luminescence instrument systems*. Radiation Measurements, 32(56): 523–528, 2000.

Chen, Y.W., Li, S.H., and Li, B. *Residual doses and sensitivity change of post IR IRSL signals from potassium feldspar under different bleaching conditions*. Geochronometria, 40: 229–238, 2013.

Chen, Y.W., Li, S.H., Li, B., Hao, Q.Z., and Sun, J.M. *Maximum age limitation in luminescence dating of Chinese loess using the multiple-aliquot MET-pIRIR signals from K-feldspar*. Quaternary Geochronology, 30: 207–212, 2015.

Duller, G.A.T. *Single-grain optical dating of Quaternary sediments: why aliquot size matters in luminescence dating*. Boreas, 37: 589–612, 2008.

Fu, X., Li, B., and Li, S H. *Testing a multi-step post-IR IRSL dating method using polymineral fine grains from Chinese loess*. Quaternary Geochronology, 10: 8–15, 2012.

Galbraith, R.F. and Roberts, R.G. *Statistical aspects of equivalent dose and error calculation and display in OSL dating: An overview and some recommendations*. Quaternary Geochronology, 11: 1–27, 2012.

Galbraith, R.F., Roberts, R.G., Laslett, G.M., Yoshida, H., and Olley, J.M. *Optical dating of single and multiple grains of Quartz from Jinmium Rock Shelter, Northern Australia: Part I, Experimental design and statistical models*. Archaeometry, 41(2): 339–364, 1999.

Guo, Y.J., Li, B., Zhang, J.F., and Roberts, R.G. *Luminescence-based chronologies for Palaeolithic sites in the Nihewan Basin, northern China: First tests using newly developed optical dating procedures for potassium feldspar grains*. Journal of Archaeological Science: Reports, 3: 31–40, 2015.

Guralnik, B., Li, B., Jain, M., Chen, R., Paris, R.B., Murray, A.S., Li, S.H., Pagonis, V., Valla, P.G., and Herman, F. *Radiation-induced growth and isothermal decay of infrared-stimulated luminescence from feldspar*. Radiation Measurements, 81: 224–231, 2015.

Li, B. and Li, S.H. *Luminescence dating of K-feldspar from sediments: A protocol without anomalous fading correction*. Quaternary Geochronology, 6(5): 468–479, 2011.

Li, B. and Li, S.H. *Luminescence dating of Chinese loess beyond 130 ka using the non-fading signal from K-feldspar*. Quaternary Geochronology, 10: 24–31, 2012.

Li, B., Jacobs, Z., Roberts, R.G., and Li, S.H. *Extending the age limit of luminescence dating using the dose-dependent sensitivity of MET-pIRIR signals from K-feldspar*. Quaternary Geochronology, 17: 55–67, 2013a.

Li, B., Roberts, R.G., and Jacobs, Z. *On the dose dependency of the bleachable and non-bleachable components of IRSL from K-feldspar: Improved procedures for luminescence dating of Quaternary sediments*. Quaternary Geochronology, 17: 1–13, 2013b.

Li, B., Jacobs, Z., Roberts, R., and Li, S.H. *Review and assessment of the potential of post-IR IRSL dating methods to circumvent the problem of anomalous fading in feldspar luminescence*. Geochronometria, 41(3): 178–201, 2014a.

Li, B., Roberts, R.G., Jacobs, Z., and Li, S.H. *A single-aliquot luminescence dating procedure for K-feldspar based on the dose-dependent MET-pIRIR signal sensitivity*. Quaternary Geochronology, 20: 51–64, 2014b.

Li, B., Roberts, R.G., Jacobs, Z., and Li, S.H. *Potential of establishing a 'global standardised growth curve' (gSGC) for optical dating of quartz from sediments*. Quaternary Geochronology, 27: 94–104, 2015a.

Li, B., Roberts, R.G., Jacobs, Z., Li, S.H., and Guo, Y J. *Construction of a 'global standardised growth curve' (gSGC) for infrared stimulated luminescence dating of K-feldspar*. Quaternary Geochronology, 27: 119–130, 2015b.

Li, B., Jacobs, Z., and Roberts, R. *Investigation of the applicability of standardised growth curves for OSL dating of quartz from Haua Fteah cave, Libya*. Quaternary Geochronology, 35: 1–15, 2016.

Li, B., Jacobs, Z., Roberts, R.G., Galbraith, R., and Peng, J. *Variability in quartz OSL signals caused by measurement uncertainties: problems and solutions*. Quaternary Geochronology, 41: 11–25, 2017.

Lian, O.B. and Roberts, R.G. *Dating the Quaternary: progress in luminescence dating of sediments*. Quaternary Science Reviews, 25: 2449–2468, 2006.

Lu, Y.C., Wang, X.L., and Wintle, A.G. *A new OSL chronology for dust accumulation in the last 130,000 yr for the Chinese Loess Plateau*. Quaternary Research, 67: 152–160, 2007.

Murray, A.S. and Roberts, R.G. *Measurement of the equivalent dose in quartz using a regenerative-dose single-aliquot protocol*. Radiation Measurements, 29: 503–515, 1998.

Murray, A.S. and Wintle, A.G. *Luminescence dating of quartz using an improved single-aliquot regenerative-dose protocol*. Radiation Measurements, 32(1): 57–73, 2000.

Panagopoulou, E., Tourloukis, V., Thompson, N., Athanassiou, A., Tsartsidou, G., Konidaris, G.E., Giusti, D., Karkanas, P., and Harvati, K. *Marathousa 1: A new Middle Pleistocene archaeological site from Greece*. Antiquity Project Gallery, 89(343), 2015.

Peng, J., Dong, Z.B., Han, F.Q., Long, H., and Liu, X.J. *R package numOSL: numeric routines for optically stimulated luminescence dating*. Ancient TL, 31: 41–48, 2013.

Peng, J., Pagonis, V., and Li, B. *On the intrinsic accuracy and precision of the standardised growth curve (SGC) and global-SGC (gSGC) methods for equivalent dose determination: A simulation study*. Radiation Measurements, 94: 53–64, 2016.

R Core Team. *R: A Language and Environment for Statistical Computing*. R Foundation for Statistical Computing, 2016. URL https://www.R-project.org/.

Roberts, H.M. and Duller, G.A.T. *Standardised growth curves for optical dating of sediment using multiple-grain aliquots*. Radiation Measurements, 38: 241–252, 2004.

Van den Bergh, G.D., Li, B., Brumm, A., Grün, R., Yurnaldi, D., Moore, M.W., Kurniawan, I., Setiawan, R., Aziz, F., Roberts, R.G., Suyono, S.M., Setiabudi, E., and Morwood, M.J. *Earliest hominin occupation of Sulawesi, Indonesia*. Nature, 529: 208–211, 2016.

Van Vugt, N., De Bruijn, H., Van Kolfschoten, T., and Langereis, C.G. *Magneto- and cyclostratigraphy and mammal-faunas of the Pleistocene lacustrine Megalopolis Basin, Peloponnesos, Greece*. Geologica Ultrajectina, 189: 69–92, 2000.

Vinken, R. *Stratigraphie und Tektonik des Beckens von Megalopolis (Peloponnes, Griechenland)*. Geologisches Jahrbuch, 83: 97–148, 1965.

Wintle, A.G. *Recent developments in optical dating of sediments*. Radiation Protection Dosimetry, 47: 627–635, 1993.

Wintle, A.G. *Luminescence dating methods*. In Holland, H D and Turekian, K K (eds.), *Treatise on Geochemistry*, pp. 17–35. Elsevier, Oxford, 2nd edition, 2014.

Reviewer

Vasilis Pagonis